

1 Published in *Agricultural Systems* (2017 IF: 3.004, 5-yr IF: 3.756), Vol. 173, pp. 94–106.

2

3 **Optimizing regional cropping systems with a dynamic adaptation strategy for**
4 **water sustainable agriculture in the Hebei Plain**

5

6 Honglin Zhong¹, Laixiang Sun^{1,2,3}, Günther Fischer², Zhan Tian⁴, Zhuoran Liang⁵

7

8 1. Department of Geographical Sciences, University of Maryland, College Park, United States;

9 2. International Institute for Applied Systems Analysis, Laxenburg, Austria;

10 3. School of Finance and Management, SOAS, University of London, London, UK;

11 4. School of Environmental Science & Engineering, Southern University of Science &
12 Technology, Shenzhen, China;

13 5. Hangzhou Meteorological Services, Hangzhou, Zhejiang, China

14

15

16 **Correspondence to:** Laixiang Sun, Email: lsun123@umd.edu, Tel: +1-301-405-8131, Fax: +1-
17 301-314-9299

18

19

20 **Acknowledgements**

21 This work was supported by the National Natural Science Foundation of China (Grant Nos.
22 51761135024, 416711113, 4160011367 and 41601049). We thank Austin Sandler and Ipsita
23 Kumar for exposition improvement.

24

25

26

27

28 **Abstract**

29 Unsustainable overexploitation of groundwater for agricultural irrigation has led to rapid
30 groundwater depletion and severe environmental damage in the semi-arid Hebei Plain of China.
31 Field experiments have recommended annual winter fallowing (i.e., forgoing winter wheat
32 production) as the most effective way to replenish groundwater. However, adopting the
33 recommendation across the Hebei Plain would lead to a significant reduction in total wheat
34 production. This research aims to find the most favorable water-sustainable cropping systems for
35 different localities in the Hebei Plain, which at the regional aggregation level maintains the
36 uppermost overall levels of wheat and grain production respectively. Our simulations indicate that
37 in the Hebei Plain, an optimal allocation of a *wheat-early maize relay intercropping system* and an
38 *early maize-winter fallow cropping system* across the Hebei Plain could lead to significant water
39 savings while minimizing grain production losses to around 11%. Compared to the prevailing
40 *wheat and summer maize cropping system*, to prevent a drop in the water table, 39% of the current
41 wheat cropping land would need to be fallowed in winter, reducing irrigation water use by
42 $2,639 \times 10^6 \text{ m}^3$. Replacing the prevailing *wheat and summer maize cropping system* with our
43 optimized allocation system could lead to a 36% increase in total maize production and 39%
44 decrease in total wheat production, resulting in total agricultural irrigation water savings of $2,322$
45 $\times 10^6 \text{ m}^3$ and a total grain production reduction by 11%. The findings indicate the potential benefits
46 of our cropping system adaptation method to meet the challenge of recovering local groundwater
47 level with the least possible reduction of wheat and total grain production in the Hebei Plain.

48

49 **Keywords:** relay intercropping system; groundwater overexploitation; cropping system
50 adaptation; water sustainable agriculture; the Hebei Plain; China

51 **1. Introduction**

52 Heavy dependence on groundwater irrigation has been the key feature of wheat production in
53 the water scarce Hebei Plain (Yuan and Shen, 2013; Hu et al., 2016), where much of China's wheat
54 is produced. Current intensive multi-cropping systems constitute about 70% of the total water use
55 in the Hebei Plain, of which 70% is consumed by wheat irrigation (Lv et al., 2013). About 400
56 mm of groundwater is required to irrigate wheat under local farmers' conventional practice (Sun
57 et al., 2011). The large amount of water demand for agricultural irrigation exceeds the renewable
58 water availability, and has led to subsequent unsustainable groundwater over-exploitation. As a
59 result, the water table has dropped rapidly from 10 meters below the land surface in the 1970s to
60 40 meters in the early 2010s (Shen et al., 2002; Zhang et al., 2011), which has caused serious
61 environmental degradation and considerable economic losses (Zhang et al., 2009). The scarcity of
62 groundwater in the Plain is alarming; and the soaring water use from industries and municipalities
63 has put additional pressure on the rapidly dropping groundwater table (Wang et al., 2009). The
64 agricultural sector in the Plain faces a two-fold challenge. On the one hand, the groundwater
65 shortage has already threatened wheat production in the Plain (Li et al., 2015), potentially
66 compromising China's food security in the near future. On the other hand, the current practice of
67 overexploiting groundwater would need to stop as soon as possible to conserve the aquifers (van
68 Oort et al., 2016).

69 The two-fold challenge of the agricultural sector has stimulated a large body of research on
70 water saving irrigation technologies, less water-intensive cropping systems, and cost-benefit
71 analyses of fallow cropland (Kang et al., 2002; Li et al., 2005; Sun et al., 2011; Yang et al., 2015;
72 van Oort et al., 2016). Under the current cropping system, even reducing the irrigation frequency
73 to one time per crop growth cycle (i.e., deficit irrigation) cannot prevent the water table from
74 dropping (Sun et al., 2015). Thus, many researchers have tried to construct alternative water-
75 sustainable cropping systems. Because of dry winter and spring, wheat growth requires much more
76 irrigation than other cereal crops in the Plain (Yang et al., 2015), alternative water-sustainable
77 cropping systems that partially or completely forgo winter wheat are suggested to replace the
78 prevailing *winter wheat-summer maize sequential cropping* (WM-S). These alternative cropping
79 systems include single cropping of spring maize (Pei et al., 2015), double cropping per year of
80 early maize and late maize (Meng et al., 2017), and triple harvests in two years of WM-S followed

81 by spring maize (Meng et al., 2012), and strip relay-intercropping of wheat followed by spring
82 maize (Gao et al., 2009).

83 The recent field experiments reported in Pei et al. (2015) revealed that early maize, which
84 moves the traditional maize sowing date earlier by 10-20 days, has a much higher water
85 productivity compared with summer maize and spring maize. Based on the productivity advantage
86 of early maize, Zhong et al. (2017) recommended a regional-scale cropping system adaptation
87 strategy for the North China Plain, which includes the Hebei Plain, under the constraints of local
88 water supply. Their recommendation would supersede the current WM-S with the *early maize-*
89 *winter fallow* (EM-F) and the *winter wheat-early maize relay intercropping* (WM-R). Their
90 recommended strategy reconciles the two-fold challenge of maintaining regional grain production
91 while recovering groundwater in the North China Plain. However, this reconciliation is a result of
92 a large-scale substitution of wheat for maize and would lead to a considerable reduction in wheat
93 production. Reduced wheat production would undermine the food security of Northern China,
94 where wheat is the number one staple food for locals. Xiao et al. (2017) presented a farm-level
95 water sustainable cropping system of triple cropping in two years, with winter wheat-summer
96 maize sequential cropping in the first 12 months followed by winter fallow and early maize in the
97 second 12 months (WM-FE), at Luancheng Agro-Ecological Experimental Station (114.41°E,
98 37.53°N) in the Hebei Plain. Their simulations using the APSIM model (Keating et al., 2003)
99 showed promising potential of the WM-FE regime to achieve neutral groundwater depletion with
100 a moderate reduction in total grain yield of 13%, but a significant wheat yield reduction of 50%
101 compared with the existing WM-S regime. However, the equilibrium of the water table depth
102 under WM-FE could not be established without two groundwater recharge sources: (1) A
103 groundwater recharge of 113 mm/year from the mountain-front recharge system, which is only
104 available in the piedmont part of the Hebei Plain (Chen et al., 2003; Hu et al., 2010; Sun and Ren,
105 2013). (2) An additional surface water recharge of 41 mm/year from the South-North Water
106 Transfer Project. An application of this site-based result to other locations would lead to a water
107 table drop by about 200 mm/year and a reduction of regional total wheat production by 50% in the
108 Hebei Plain (Luo et al., 2018).

109 Although the adaptation strategies suggested by Zhong et al. (2017) and Xiao et al. (2017)
110 were unable to avoid significant reduction in wheat production, a combination of the
111 complementary advantages of WM-R in higher yield and EM-F in water savings may allow us to

112 develop an optimal allocation method; one that achieves local groundwater equilibrium and
113 minimizes the reduction of total wheat production in the Hebei Plain. Our method also considers
114 other various existing multi-cropping systems along with the water usage of various crops,
115 vegetables, and fruit trees. To facilitate the design and assess the performance of our method, we
116 employ DSSAT 4.6 to simulate the crop growth processes and the associated evapotranspiration
117 levels of the WM-S, WM-R and EM-F regimes under the optimal irrigation schedules presented
118 in Sun et al. (2011). Owing to the lack of field observation data and the limitations in scope of the
119 DSSAT model, we employ AEZ v3.0 to simulate the evapotranspiration levels in each growing
120 stage of other crops, vegetables and fruit trees.

121 Our results demonstrate that it is possible to meet the two-fold challenge in the Hebei Plain of
122 maintaining regional grain production while stopping overexploitation of groundwater. The
123 spatially explicit winter-wheat sacrificing strategy demonstrated in this research provides support
124 to future agricultural policy designs aiming to recover groundwater in the Plain.

125

126 **2. Study Region**

127 The Hebei Plain (113.5°E–117.8°E, 36.0°N–39.5°N) is located in the northern part of the North
128 China Plain, bounded by the Taihang Mountains on the West and Bohai Sea on the East (Figure
129 1). It includes 84 counties, covers a total area of 61,636 km², and has a semi-arid monsoon climate
130 with average annual temperatures of 12-13°C and 450-600 mm of annual precipitation. Seasonal
131 precipitation is highly variable, with about 80% of the annual precipitation occurring in the
132 summer (June to September), and less than 20% occurring in winter and spring. The local thermal
133 resource is sufficient for sequential cropping systems of two harvests in one year or three harvests
134 in two years. In the Hebei Plain, WM-S is the prevailing cropping system. Farmers cultivate
135 summer maize from mid-June to late September, while sow winter wheat in early October and
136 harvest it in early June in the following year.

137 The Hebei Plain is divided into three zones: the piedmont, central, and coastal plain. The
138 piedmont plain has relatively more plentiful groundwater resources than its central and coastal
139 counterparts because of the mountain-front recharge, waterbody leakage (reservoir), and
140 groundwater lateral flow. The once abundant groundwater resources of the shallow aquifer and
141 better soil conditions made the piedmont plain the most suitable zone for irrigation expansion, and
142 has the highest cropland irrigation ratio among the three zones. However, persistent groundwater

143 over-pumping has led to a precipitous drop in the water table at an annual rate of 0.3-1.3 meters.
144 The fastest drop has been in the Shijiazhuang-Baoding irrigation district of the piedmont plain. In
145 contrast, groundwater resources for most of the central and coastal plains are limited and stored
146 deep within the aquifer. The brackish groundwater in the shallow aquifer of the coastal plain is
147 typically not suitable for crop irrigation because of the high soil salinization risk. Groundwater
148 recharge from rivers, lakes, and wetlands has reduced significantly because surface water flow to
149 the central and coastal plains is often cutoff by reservoirs built upstream, especially during the dry
150 seasons. Limited groundwater availability constrains cropland irrigation expansion in these
151 regions. On the other hand, continuous over-pumping of the limited freshwater resources has
152 caused the deep groundwater level to rapidly drop. Groundwater depletion has triggered
153 considerable seawater intrusion in the coastal region. The deepest groundwater level is 100 meters
154 below the mean seawater level (Foster and Perry, 2010), The Cangzhou irrigation district of the
155 coastal plain has been especially affected.

156

157 *(Figures 1 and 2 are about here)*

158

159 **3. Data and Methodology**

160 **3.1 Data**

161 Input data to run the DSSAT model and AEZ model includes daily weather, soil profiles, land
162 use map, wheat and maize cropping management information, and irrigated versus rainfed land
163 for all crops and fruit trees that grow in the Hebei Plain.

164 A historical daily weather dataset (2000-2010) of the Hebei Plain was taken from the
165 observation-based WATCH Forcing Data methodology to ERA-Interim data (WFDEI) product
166 (Weedon et al., 2014), with a spatial resolution of 0.5 degrees. Meteorological variables of daily
167 minimum and maximum temperature, Downward Shortwave Radiation flux, rainfall and snowfall
168 rates were used to generate the weather dataset required by the DSSAT model. In addition, wind
169 speed and relative humidity data were used to meet the requirements of the AEZ model.

170 The cropland map of the Hebei Plain in 2000 was extracted from the National Land Cover
171 database provided by the Institute of Geographical Sciences & Natural Resources Research
172 (IGSNRR) of the Chinese Academy of Sciences, with a spatial resolution of 100 meters. Cropland
173 was further divided into four sub-types: plain cropland, hilly cropland, mountain cropland, and

174 cropland with slope greater than 25 degrees. Only plain cropland was considered suitable for the
175 WM-R in this study, and WM-S on other cropland sub-types would be partially or completely
176 replaced by EM-F to reach water balance. The soil profile dataset, employed as a DSSAT model
177 input and required by the AEZ model, was obtained from the Harmonized World Soil Database
178 (HWSD) (Fischer et al., 2008), with a spatial resolution of 1 km. Additional soil properties not
179 covered by the HWSD, but required by the DSSAT model, were retrieved using the methods
180 described in Tian et al. (2014).

181 Crop-specific, irrigated and rainfed harvest areas of wheat, maize, and all other crops in the
182 Hebei Plain grown in 2000 were obtained from the MICRA2000 database (Portmann et al., 2010).
183 It provided monthly irrigated and rainfed area measurements for 26 crops grown in 2000, with a
184 spatial resolution of 5 arc minutes (about 9.2 km in the Hebei Plain). The harvest area database is
185 capable of representing multi-cropping systems and maintains consistency by construction with
186 the census-based agricultural statistics from the National Bureau of Statistics of China. This dataset
187 has been successfully applied to estimate water consumption change caused by changing the area
188 sown to winter wheat in the North China Plain (Wang et al., 2015). Figure 2 shows that the area
189 ratios of irrigated wheat, irrigated maize and rainfed maize to the county's total cropland were
190 much higher for wheat and moderately higher for maize in the piedmont than in the central and
191 coastal plains. The observed pattern was a result of lateral flow recharge from the Taihang
192 Mountains on the west of Hebei Plain in combination with better soil condition and richer shallow-
193 groundwater resources there (Mo et al., 2006).

194 All DSSAT inputs were resampled into grid cells with a spatial resolution of 1 km.

195

196 3.2 DSSAT model

197 The DSSAT model was developed by the International Benchmark Sites Network for Argo-
198 technology Transfer project (IBSNAT). It simulates the growth and development of crops within
199 a uniform plot of cropland under precise or assumed field management conditions on a daily basis.
200 It also simulates changes in water, carbon, and nitrogen levels in the soil associated with crop
201 growth and development (Jones et al., 2003). The performance of the DSSAT model in simulating
202 soil water balance, crop growth and yield had been validated with field observations at Luancheng
203 site in Hebei Plain (Yang et al., 2006) and Yingke site in Northwest China (Jiang et al., 2016). The
204 DSSAT model was employed to quantify the amount of irrigation water savings required to stop

205 groundwater drawdown under the prevailing WM-S regime in the Shijiazhuang Irrigation District
206 of Hebei Plain (Hu et al., 2010).

207 The soil-water balance module in the DSSAT model simulates the soil-water processes and the
208 soil-water content in all soil profiles (Ritchie, 1985). Daily soil-water balance is calculated using
209 precipitation, infiltration, runoff, soil transpiration, plant evaporation, and drainage during the crop
210 growth period (Jones et al., 2003), presented in Eq. 1.

$$211 \quad \Delta S = P + I - ET - R - D \quad (1)$$

213 In Eq. 1, ΔS is the net change in soil water content. P , I , ET , R , and D denote precipitation (water
214 resources), effective irrigation, evapotranspiration, surface runoff, and drainage from the soil
215 profile, respectively. All inputs and results are in mm. The local water resource change, which is
216 the difference between water recharge (i.e., drainage: D) and water extraction (i.e., effective
217 irrigation: I), is expressed as:

$$218 \quad D - I = P - ET - R - \Delta S \quad (2)$$

219 To estimate local groundwater resource change across grid-cells in a large region using the
220 DSSAT model, previous studies have employed several critical assumptions: (1) Surface runoff
221 can be neglected ($R = 0$) for the regional scale assessment due to the dried off of the surface, high
222 soil infiltration, flat topography, and small cropland parcels in the North China Plain (Yang et al.,
223 2015). (2) Soil moisture storage can be considered stable and soil moisture change is negligible
224 ($\Delta S = 0$) in this Plain (Moiwo et al., 2009, 2010), because large-scale intensive irrigation and the
225 lack of long-term drying trends in the root-zone. (3) Due to the lack of reliable observational data
226 on groundwater lateral flow, surface water flow and distribution of wells in the piedmont plain,
227 the mountain-front recharge from the Taihang Mountains in the piedmont plain and vertical
228 infiltration from waterbodies are not considered in the regional simulation (Chen et al., 2010).
229 Nevertheless, we believe mountain-front recharge and vertical infiltration may still benefit
230 groundwater recovery. Therefore, the local water resource change is expressed as:

$$231 \quad D - I = P - ET \quad (3)$$

232 In Eq. 3, P and ET refer to the local water resource and the crop water consumption
233 (evapotranspiration). Local water balance is achieved if $D - I = P - ET = 0$. Because the DSSAT
234 model can simulate water consumption (ET) of different cropping systems and precipitation (P) is
235 available from the regional climate dataset, we use $P - ET$ to calculate the local water resource

236 change (or Irrigation Water Requirement, $IWR = P - ET$) under different cropping systems during
237 the study period.

238 The total Irrigation Water Requirement (IWR_{total}) from the annual harvested area of winter
239 wheat, summer maize, and early maize under irrigated condition was calculated using the equation
240 from Yang et al. (2010):

$$241 \quad IWR_{total} = \sum_{i=1}^n IWR_i \times AR_i \quad (4)$$

242 Where IWR_i refers to the Irrigation Water Requirement of crop i during the crop growth period,
243 which includes winter wheat, summer maize, and early maize. And AR_i is the irrigated area of
244 wheat and maize in each grid cell. Irrigation water requirement of each cropping system (WM-S,
245 WM-R, EM-F) was simulated at a daily step under a given crop calendar and irrigation condition.

246 The DSSAT wheat and maize models have been widely applied in the Plain (Figure 1). Yang
247 et al. (2006) calibrated and validated the performance of the DSSAT wheat and maize models at
248 the Luancheng experimental station (114.68°E, 37.88°N). They obtained the genetic coefficients
249 of local winter wheat and summer maize varieties via DSSAT calibration and then employed these
250 coefficients to simulate the total crop irrigation water use and soil water balance. Zhong et al.
251 (2017) calibrated the DSSAT-maize model and obtained the genetic coefficients of early maize
252 based on the field observations of intercropped early maize in the Tangyin agro-meteorological
253 observation station (114.24°E, 36.03°N) and the shading algorithm developed by Knorz et al
254 (2011) for the wheat-maize co-growing period. Among 10 agro-meteorological observation
255 stations in the North China Plain that have valid records of wheat-maize multiple cropping,
256 Tangyin station is the only one with valid records for the WM-R system. Table 1 presents the
257 cultivar coefficients of local wheat, summer maize and early maize varieties. For other crops,
258 vegetables, and fruit trees planted in the Hebei Plain, we employed the simple soil-water balance
259 module of the AEZ model to simulate their water use. This is because the DSSAT model could
260 not cover all crops in the Plain, and the model calibration requires detailed field observations,
261 which were difficult to obtain for other crops and vegetables.

262

263 (*Table 1 is about here*)

264

265

266 3.3 AEZ model

267 The AEZ 3.0 model was employed to estimate the evapotranspiration of non-wheat and non-
268 maize crops. The AEZ model was jointly developed by the International Institute for Applied
269 Systems Analysis (IIASA) and the Food and Agriculture Organization (FAO) of the UN
270 (IIASA/FAO, 2012). It uses the prevailing climate resources, soil profile and topography
271 conditions, and detailed agronomic-based knowledge to simulate crop productivity and soil water
272 balance with standardized soil-plant-atmosphere interaction algorithms. Such standardized
273 methodologies make the AEZ well suited for crop productivity assessment at the regional level
274 where detailed and spatially explicit input data are relatively limited (Tubiello and Fischer, 2007;
275 Gohari et al., 2013). The AEZ model has been successfully applied to estimate the actual
276 evapotranspiration (ET_a) of wheat and maize in the Hebei Plain (Wang et al., 2015). The equation
277 to estimate the ET_a is as follows:

278

$$ET_a = \begin{cases} ET_0 \times K_c & \rho = 1 \\ P + \rho \times ET_0 \times K_c & \rho < 1 \end{cases} \quad (5)$$

279 Where ET_0 refers to the reference crop evapotranspiration, which is calculated using the widely
280 applied Penman-Monteith equation (Allen et al., 1998). K_c refers to the crop coefficients, which
281 varies in different crop growth stages. The K_c coefficients for all other crops are obtained from
282 FAO (Allen et al., 1998). P is the daily precipitation. ρ refers to the soil-water coefficient in the
283 AEZ model. If the current water balance is greater than or equal to the threshold of readily available
284 soil water, then $\rho = 1$. If the permanent wilting capacity is less than the current water balance, and
285 the current water balance is less than the readily available soil water, then $0 < \rho < 1$. If the current
286 water balance is less than the permanent wilting capacity, then $\rho = 0$ (IIASA/FAO, 2012; Wang et
287 al. 2015).

288 Because not all of the crops in the MICRA2000 dataset were planted in the Hebei Plain, and
289 there was a mismatch of the crop types between the AEZ model and the MICRA2000 dataset, we
290 grouped crops planted in the Hebei Plain into 14 groups (rice, barley, rye, millet, sorghum, soybean,
291 sunflower, potato, sugar cane, sugar beet, groundnut, citrus/fruit tree, cotton, cabbage/vegetables).
292 The evapotranspiration of fruit trees (other than citrus) were calculated with the Pan-ET method
293 using the Pan-evaporation coefficient from Yang et al. (2010). The Pan-ET method derives
294 evapotranspiration by,

295

$$296 \quad ET_i = \lambda_i \times ET_{pan} \quad (6)$$

297

298 where ET_i is the actual evapotranspiration, and λ_i is the pan-evaporation coefficient for fruit tree
299 *i*. ET_{pan} is the local observations of evapotranspiration from a 200 mm diameter evaporation pan
300 in the meteorological stations in the Hebei Plain.

301 It is worth noting that the estimation of evapotranspiration played a central role in this research.
302 We ensured that evapotranspiration estimates were compatible across the DSSAT model, the AEZ
303 model, and the Pan-ET method, as all of them used the same Penman-Monteith equation (Allen et
304 al., 1998) for the estimates.

305

306 3.4 Cropping system adaptation strategy

307 Using a loop method (Figure 3), we established our cropping system adaptation strategy to keep
308 total local agricultural water consumption within the limits of the local water resource. It replaces
309 the current WM-S with WM-R or EM-F across the grid-cells within each county of the Hebei Plain.
310 For other crops, vegetables, and fruit trees, we assumed that their areas and planting locations
311 remained the same, as did their evapotranspiration. The WM-R and EM-F cropping area were
312 dynamically allocated within the WM-S occupied grid-cells. Our aim was to achieve local water
313 balance under the constraint of minimizing the reduction in wheat production and subsequently
314 total grain production in each county. The reason for doing the initial balance loop at the county
315 level is as follows. Our simulated balance loop experiments for the whole of the Hebei Plain led
316 to significantly higher reductions of wheat production in comparison with the simulated balance
317 loop experiments within each county. In more detail, for the whole of the Hebei Plain, completely
318 forgoing winter wheat results in excessive water saving in the northern Hebei Plain to compensate
319 for water over-consumption in the southern Hebei Plain; whereas at the county level, partially
320 forgoing winter wheat to lower groundwater exploitation-discharge balances out within each
321 county. The intuition is that while there were no significant lateral water flows across the three
322 sub-plains, at the intermediate scale of a county, it becomes more likely for groundwater to be
323 balanced via lateral underground water flow from the areas with a higher water table (groundwater
324 recovery) to the areas with a lower water table (groundwater overdraft), as shown in Figure 11 of

325 Kendy et al. (2003). Therefore, we applied the cropping system allocation method across grid-cells
326 within each county.

327 Major steps of the allocation method (Figure 3) are: (1) At the grid-cell level, we estimated the
328 evapotranspiration of the WM-R, WM-S, EM-F regimes under an optimal irrigation schedule
329 using the DSSAT model; and estimated the evapotranspiration of other crops, vegetables, and fruit
330 trees using the AEZ model and the Pan-ET method. (2) We identified the areas of existing planting
331 systems —*wheat and summer maize cropping system (WM-S)*, *wheat-other crops multi-cropping*
332 *system*, and *other cropping systems*—based on the existing wheat and maize cropping areas within
333 each grid cell. We assumed that land occupied by other crops, vegetables, and fruit trees would
334 remain unchanged, and that fallowing might replace wheat in the areas occupied by the *wheat-*
335 *other crops multi-cropping system* to save water. (3) At the grid-cell level for a given county, we
336 calculated the *remaining total water resource* from the total water supply from precipitation less
337 the total evapotranspiration of the *winter fallow-other crops multi-cropping systems* and all other
338 cropping systems not including the *wheat-maize multi-cropping system*. We then sorted all grid
339 cells in ascending order according to their *remaining total water resource*. (4) Using the algorithm
340 developed by Zhong et al., (2017), we estimated the baseline of WM-R and EM-F allocations
341 under the constraint of no loss in total grain production within each county. We then compared the
342 total evapotranspiration of the adaptive cropping systems (WM-R and EM-F) to the ascending list
343 of *remaining total water resources*. (5) If the evapotranspiration from the adaptive cropping
344 systems is less than the *remaining total water resource*, then using more water would increase
345 wheat production. We then replaced EM-F with WM-R starting from the grid-cell with highest
346 *remaining total water resource*. If the evapotranspiration from the adaptive cropping systems is
347 greater than the *remaining total water resource*, then fallowing wheat fields would increase water
348 savings. We then replaced WM-R with EM-F starting from the grid-cell with lowest *remaining*
349 *total water resource*. We perform this final adjustment to balance the agricultural water use and
350 groundwater recharge within a county. We repeated steps 3-5 for each county in the Hebei Plain.
351 (6) Finally, we compared the adaptive cropping systems to the existing wheat and maize cropping
352 systems in the Hebei Plain, to measure the impact on grain production, fallowed area extent, and
353 groundwater flows.

354

355 (Figure 3 is about here)

356

357 3.5 Crop management and DSSAT model upscaling

358 Regional crop production and evapotranspiration across the Hebei Plain were simulated using
359 the DSSAT model up-scaling method (Tian et al., 2012) with local wheat, maize and early maize
360 cultivars (Yang et al., 2006; Zhong et al., 2017). The local summer maize sowing dates in the
361 Hebei Plain under the WM-S were obtained from Figure 2 in Binder et al. (2008), which were
362 based on observations from 14 agro-meteorological stations in the North China Plain. Summer
363 maize was sown right after the harvest of wheat, and wheat was sown 10 days after the harvest of
364 maize for land preparation. In contrast, under the WM-R and EM-F, early maize was sown 15 days
365 before the existing wheat harvest date (Zhong et al., 2017).

366 Optimal wheat and maize irrigation schedules, as developed by Sun (2011), were applied to
367 reduce the irrigation water amount, and automatic irrigation was selected in the DSSAT model to
368 maintain the soil moisture between 45% and 80% of soil water capacity during the critical wheat
369 growing stages. Maize was irrigated during germination and the jointing stage in the case of dry
370 weather condition (Pei et al., 2015; Sun et al., 2011). The optimal crop management was applied
371 with the absence of weeds, no pests and diseases, and no nutrient constraint. 100 kg of nitrogen
372 fertilizer was applied at sowing and stem elongation to ensure no nitrogen limitation during the
373 crop growth period (Wang et al., 2012). Therefore, the wheat and maize yield were the attainable
374 yields under optimal crop irrigation and management conditions.

375

376 **4. Results**

377 4.1 Evapotranspiration under existing cropping systems

378 The evapotranspiration of wheat, summer maize, and early maize under optimal irrigation
379 schedule, and the evapotranspiration of other crops and fruit trees under the existing regional
380 cropping systems are estimated using the DSSAT model, the AEZ model, and the Pan-ET method.
381 Table 2 reports the aggregate evapotranspiration of wheat, maize, and the combination of other
382 crops, vegetables, and fruit trees across the three plains. And Figure 4 depicts the spatial
383 distribution of their evapotranspiration shares. As shown in Table 2, wheat and maize account for
384 28% and 23% of the total evapotranspiration in the Hebei Plain. In the piedmont plain where the
385 area share of wheat and maize is the highest among the three plains, wheat and maize together
386 account for 56% of the total evapotranspiration. In contrast, the evapotranspiration shares of wheat

387 and maize in the central and coastal plains are smaller than the evapotranspiration share of other
388 crops, vegetables, and fruit trees combined.

389

390 (*Table 2 and Figure 4 are about here*)

391

392 4.2 Areas for wheat fallow and *wheat-early maize relay intercropping system* (WM-R)

393 In Table 3 we present the aggregate results for winter wheat fallow areas and the potential of
394 WM-R. And Figure 5 shows the spatial distribution of winter wheat fallow areas compared with
395 existing wheat cropping areas, and WM-R compared to the existing WM-S cropping area, at the
396 county-level. Table 3 shows that compared with the central and coastal plains, the piedmont plain
397 has the highest ratio of wheat fallow land to the existing wheat land (45%). The disparity is because
398 of the higher area-share of wheat in the county's total cropland and the greater Irrigation Water
399 Requirement of wheat in the piedmont plain. Some counties in the piedmont plain would even
400 need to fallow about 70% of their wheat cropped land to achieve water balance. In contrast, about
401 36% and 33% of the wheat cropped land would need to be fallowed in the central and coastal
402 plains, especially in the southern part of the Hebei Plain. The central plain becomes the preferred
403 location to fallow because wheat cropped land in the central plain is much larger than the piedmont
404 and coastal plains.

405 Our results in Figure 5 and Table 3 also indicate that WM-R would be the dominant cropping
406 system under our adaptation strategy. Thus, 72%, 76%, and 68% of the existing WM-S area in the
407 three sub-plains will be replaced by WM-R in order to minimize the reduction of both the total
408 wheat production and the total grain production. Figure 5 shows that counties in the southern Hebei
409 Plain would have a larger portion of their existing WM-S cropping area replaced by WM-R due to
410 the smaller ratio of fallowed land to the existing wheat land. Whereas, counties with a high ratio
411 of fallowed land would be located in the middle of the piedmont plain and central plain. The
412 relatively smaller portion of their existing WM-S cropping land would need to adopt WM-R.

413

414 (*Table 3 and Figure 5 are about here*)

415

416 4.3 Regional grain production and Irrigation Water Requirement (IWR) change

417 Table 4 shows the changes in the potential production of wheat, maize, and the regional total
418 grain production between our adaptive cropping systems and the existing cropping systems in the
419 Hebei Plain. It shows that the total wheat production in the piedmont, central and coastal plain
420 would be 45%, 36% and 33% less than that under the existing cropping system, respectively. This
421 implies that our wheat fallow strategy may lead to a total reduction in wheat production of 39% in
422 the Hebei Plain, which is smaller than about 50% under WM-FE (at Luancheng site in Xiao et al.
423 2017 and at the regional level of the Hebei Plain in Luo et al 2018, without considering water-
424 balance of the whole cropping sector) and 100% under EM-F. On the other hand, adopting early
425 maize may increase total maize production by about 35%, 37% and 36% in the piedmont, central
426 and coastal plains, respectively, and this means that the reduction in total production of wheat and
427 maize in the three plains would be decreased to the level of 16%, 9% and 3% respectively. For the
428 Hebei Plain as a whole, total early maize production would increase by 36%, and the total grain
429 production would suffer a moderate 11% reduction

430 The spatial distribution of the wheat production reduction (see Figure 6) is highly depended on
431 the area ratio of fallowed wheat (see Figure 5), because most of the wheat is irrigated in the Hebei
432 Plain. To various extents, all counties may suffer a reduction in wheat production as a result.
433 Generally speaking, there would be a greater increase in maize production in the south than in the
434 north; which is mainly due to higher precipitation, better thermal resources, and earlier sowing
435 dates of maize during the summer in the south. Although the irrigated maize area in the south
436 Hebei Plain is smaller than in the north, our results indicate that adopting early maize may lead to
437 more maize production in the south. For some counties located in the north piedmont plain, east
438 central plain, and coastal plain, maize production gains would be smaller than in the rest of the
439 Hebei Plain, due to maize growth more often under rainfed conditions during the summer.

440 The IWR changes in each county across the Hebei Plain (Figure 6) and the total IWR changes
441 across the three plains (Table 5) are also estimated. The total IWR change of wheat and maize is
442 determined by total wheat fallow area and irrigated early maize cropping area in each county. The
443 IWR reduction from wheat fallow is the highest in the north piedmont plain and the central plain,
444 where the area ratio of fallowed land is the highest. Similarly, the IWR increase from replacing
445 summer maize with early maize is also the highest in the north piedmont plain and the central plain
446 because of the share of existing irrigated maize cropping area is the highest there (Figure 2).
447 Aggregated results shown in Table 5 indicate that forgoing winter wheat may reduce the total

448 wheat IWR by 63%, 61% and 42% in the piedmont, central and coastal plain, respectively, a saving
449 in total IWR of $2,638.88 \times 10^6 \text{ m}^3$ for the Hebei Plain as a whole. On the other hand, replacing
450 summer maize with early maize would lead to an IWR increase by 30%, 41% and 23% in the three
451 plains respectively, an increase in total IWR of $316.95 \times 10^6 \text{ m}^3$. Taking together the above IWR
452 saving and increase, the total IWR in the Hebei Plain would decrease by 44% ($2321.93 \times 10^6 \text{ m}^3$),
453 which would contribute significantly to the groundwater recovery in the Plain.

454

455 (*Tables 4-5 and Figures 6-7 are about here*)

456

457 **5. Conclusions and Discussions**

458 The ongoing water crisis in the semi-arid Hebei Plain, driven by rapid urbanization and
459 irrigation-intensive agricultural systems, has raised public concerns in recent years. Agricultural
460 irrigation, which relies heavily on groundwater and consumes more than 70% of the total regional
461 water use, has received special attention in the Hebei Plain (Lv et al., 2013). A number of
462 groundwater sustainable cropping systems and water saving irrigation technologies have been
463 tested in field experiments, with the aim to optimize field irrigation water management and recover
464 the groundwater table. However, the field experiments all exhibit significant costs in wheat
465 production loss. The significant loss of wheat production would threaten the wheat supply of the
466 northern Chinese population, for whom wheat has been the most important staple food. To
467 overcome the limitations of the existing adaptation proposals, we propose a dynamic adaptation
468 strategy in this research to identify water sustainable cropping systems, with the minimum
469 production loss of wheat and regional grain production overall. Our strategy takes advantage of
470 two alternative cropping systems: *early maize-winter fallow cropping system* to save water, and
471 *wheat-early maize relay intercropping system* to increase grain production. And our strategy is
472 subject to the local constraints at the county level of water balance, climate, soil, water resources,
473 and existing cropping systems for other crops, vegetables, and fruit trees. Results of our
474 simulations using the DSSAT and AEZ models demonstrate that our cropping system adaptation
475 strategy may potentially reduce irrigation water consumption by up to $2,321.93 \times 10^6 \text{ m}^3$, and
476 minimize the penalty of wheat production loss to 39% and total grain production loss to 11%. This
477 level of reduction in wheat and total grain production is much less than comparable figures
478 reported in the alternative cropping system adaptation proposals (see Xiao et al., 2017; Luo et al,

479 2018). In this way, our simulated scenarios may help prevent ecological disasters from the
480 alarming groundwater crisis, and help to ensure food security for the Chinese population.

481 To make the newly proposed dynamic cropping system adaptation strategy more practical for
482 local farmers, income compensation policies for fallow cropland, enforceable regulations and
483 pricing for irrigation water use, skill training of water saving irrigation technologies, and
484 mechanization of relay intercropping are necessary (Webber et al., 2008; Feike et al., 2012).
485 Currently, farmers in the Hebei Plain have limited incentive to save irrigation water largely
486 because the pumping of groundwater is constrained only by pumping costs. Great effort should be
487 made to draw the attention of the local farmers to groundwater conservation, and more
488 fundamentally to encourage them to participate in fallowing winter wheat (Wu and Xie, 2017).
489 Income compensation policies with subsidies transferred from the urban sectors to local farmers
490 would greatly promote the willingness of local farmers to abandon winter wheat planting. To
491 encourage the adoption of the *wheat-early maize relay intercropping system*, specialized machines
492 for early maize sowing in row between wheat are needed. In this regard, the “interseeder” machine
493 designed for row relay intercropping of wheat-soybean (Feike et al., 2012) could be adapted for
494 row intercropping of the *wheat-early maize relay intercropping system*.

495 Many people have advocated that groundwater should be priced in line with its scarcity so as
496 to induce an economic mechanism that would facilitate the sustainable use of groundwater for
497 irrigation (Anderson and Leal, 2001; Nyberg and Rozelle, 1999; Wang et al., 2016; Zhang and
498 Zhang, 1995). However, the literature review of Kendy et al. (2003) indicated that such a pricing
499 policy change is not necessarily beneficial to the North China Plain, and may impose an undue
500 financial burden on already cash-strapped farmers without solving the intended problem. They
501 argued that higher prices could be justified only if water pricing encourages land-use change.
502 Congruent with their argument, our research findings provide a useful recommendation for future
503 water-pricing policy designs in the Hebei Plain. Namely, to promote the allocation of the *wheat-
504 early maize relay intercropping system* and the *early maize-winter fallow cropping system*.

505 In addition to reducing irrigation water use for wheat and maize, our simulations of total water
506 consumption in terms of evapotranspiration indicate that it is important to improve the water use
507 efficiency of other crops, vegetables, and fruit trees, and to increase infrastructure investment for
508 highly water-efficient vegetable production via rainwater harvesting and recycle use of water in
509 green houses. Previous studies have focused on optimizing irrigation water management and water

510 use efficiency of wheat and maize in the piedmont plain. As shown by our simulations and Yang
511 et al. (2010), reducing the irrigation of other crops, vegetables, and fruit trees should be considered
512 in future research because they consume nearly 50% of the total irrigation water in the Hebei Plain.
513 More studies at both site-specific and regional scales should be constructed also to identify detailed
514 water saving measurements and strategies for other crops, vegetables, and fruit trees.

515 Despite the usefulness of both the DSSAT and AEZ models in quantifying the amount of
516 Irrigation Water Requirement and soil water balance based on crop growth, crop management, and
517 climate conditions (Yang et al., 2006; Wang et al., 2015), several limitations of our simulations
518 should be specified. First, our simulations are unable to incorporate additional groundwater
519 recharge from ponds and rivers, drainage water from surface water runoff in the central plain, and
520 underground lateral aquifer flow from the Taihang Mountains. Second, because both the DSSAT
521 and the AEZ models simulate only the soil water balance in the root zone during the crop growing
522 cycle, to further assess the impact of irrigation volume change on groundwater variability and to
523 include additional groundwater recharge sources requires integration of crop-growth models and
524 physical hydrological models (Nakayama et al., 2006; Hu et al., 2010; Shu et al., 2012) or machine
525 learning models (Guzmán et al., 2017). Unfortunately, the integrated crop-hydrology models
526 require very large data inputs for model calibration and up-scaling to the regional scale. Moreover,
527 the existence of numerous dams and wells makes it cost prohibitive to collect detailed data across
528 the region to meet the data requirements of the integrated modeling. Third, although the radiation
529 interception effect on crop growth and yield during the co-growth period of wheat and early maize
530 has been successfully integrated into the DSSAT model, crop transpiration and soil evaporation
531 change during this co-growth period are still unclear due to the lack of field observations on soil
532 temperature and wind speed change during the period (Knorzer et al., 2011). Total
533 evapotranspiration may be slightly overestimated, although only for 15 days at the early stage of
534 maize growth.

535 Our agricultural adaptation strategy may have beneficial implications for other major cropping
536 regions, which face the same challenge of rapid groundwater depletion, in North America, South
537 Asia, North Africa and Middle East (Konikow and Kendy, 2005; Aeschbach-Hertig and Gleeson,
538 2012). For example, the Indo-Gangetic Plains (IGP) in India, where severe groundwater depletion
539 has occurred because of the water-intensive wheat-rice double cropping system and irrigated
540 cropland expansion (Zaveri et al., 2016). Similar to the Hebei Plain in China, the summer dominant

541 rainfall monsoon climate in the IGP leads to excessive groundwater irrigation requirements for
542 wheat during the dry winter seasons (Biemans et al., 2016). Besides, proposed field measurements
543 could not reconcile the conflicts between grain production and groundwater recovery in the IGP:
544 site-focused conservation measurements could not stop the groundwater depletion, and
545 agricultural de-intensification will lead to grain production reduction (Bhatt et al., 2016; Balwinder
546 et al., 2015). The similarities between the IGP and Hebei Plain, suggests that our approach to
547 search for a dynamic adaptation strategy could produce a more environmentally sustainable
548 solution to achieve the balance between food security and groundwater recovery in the IGP in
549 India too. On the other hand, it is worth noting that the accuracy of similar regional studies in
550 either China or other regions of the world are highly depended on the data availability in hydrology,
551 agriculture and climate observations and on multiple-model integration across crop model,
552 hydrology model and climate model. More research work in the future is needed to address the
553 accuracy issue.

554

555

556

557 **References**

- 558 Aeschbach-Hertig, W. and Gleeson T. (2012). "Regional strategies for the accelerating global problem of
559 groundwater depletion." *Nature Geoscience* 5(12): 853-861.
- 560 Allen R., Pereira L., Raes D., et al. (1998). "Crop evapotranspiration-Guidelines for computing crop
561 water requirements-FAO Irrigation and drainage paper 56." FAO, Rome 300 (9): D05109.
- 562 Anderson T.L., Leal D.R. (2001). Priming the invisible pump. In *Free Market Environmentalism*. New
563 York: Palgrave. 89-105.
- 564 Balwinder S., Humphreys E., Gaydon D., et al. (2015). "Options for increasing the productivity of the
565 rice-wheat system of north west India while reducing groundwater depletion. Part 2. Is
566 conservation agriculture the answer?" *Field Crops Research* 173: 81-94.
- 567 Bhatt R., Kukal S., Busari M., et al. (2016). "Sustainability issues on rice-wheat cropping system."
568 *International Soil and Water Conservation Research* 4(1): 64-74.
- 569 Biemans H., Siderius C., Mishra A., et al. (2016). "Crop-specific seasonal estimates of irrigation-water
570 demand in South Asia." *Hydrology and Earth System Sciences* 20(5): 1971-1982.
- 571 Binder J., Graeff S., Link J., et al. (2008). "Model-based approach to quantify production potentials of
572 summer maize and spring maize in the North China Plain." *Agronomy Journal* 100 (3): 862-873.
- 573 Chen C., Wang E. and Yu Q., (2010). "Modelling the effects of climate variability and water management
574 on crop water productivity and water balance in the North China Plain." *Agricultural Water
575 Management* 97 (8): 1175-1184.
- 576 Chen J., Tang C., Shen Y., et al. (2003). "Use of water balance calculation and tritium to examine the
577 dropdown of groundwater table in the piedmont of the North China Plain (NCP)." *Environmental
578 Geology* 44 (5): 564-571.
- 579 Feike T., Doluschitz R., Chen Q., et al. (2012). "How to Overcome the Slow Death of Intercropping in the
580 North China Plain." *Sustainability* 4 (10): 2550-2565.
- 581 Fischer, G., Nachtergaele F., Prieler S., et al. 2008. *Global Agro-ecological Zones Assessment for
582 Agriculture (GAEZ 2008)*. IIASA, Laxenburg, Austria and FAO, Rome, Italy.
- 583 Foster S., and Perry C., (2010). "Improving groundwater resource accounting in irrigated areas : a
584 prerequisite for promoting sustainable use." *Hydrogeology Journal* 18 (2): 291-294.
- 585 Gao Y., Duan A., Sun J., et al. (2009). "Crop coefficient and water-use efficiency of winter wheat/spring
586 maize strip intercropping." *Field Crops Research* 111 (1): 65-73.
- 587 Gohari A., Eslamian S., Abedi-Koupaei J., et al. (2013). "Climate change impacts on crop production in
588 Iran's Zayandeh-Rud River Basin." *Science of the Total Environment* 442: 405-419.
- 589 Guzmán S., Paz J., Tagert M., et al. (2018). "An integrated SVR and crop model to estimate the impacts
590 of irrigation on daily groundwater levels." *Agricultural Systems* 159: 248-259.
- 591 Hu X., Shi L., Zeng J., et al. (2016). "Estimation of actual irrigation amount and its impact on
592 groundwater depletion: A case study in the Hebei Plain, China." *Journal of Hydrology* 543: 433-
593 449.
- 594 Hu Y., Moiwo J., Yang Y., et al. (2010). "Agricultural water-saving and sustainable groundwater
595 management in Shijiazhuang Irrigation District, North China Plain." *Journal of Hydrology* 393
596 (3-4): 219-232.
- 597 IIASA/FAO (2012). *Global Agro-Ecological Zones (GAEZ 3.0)*. IIASA, Laxenburg, Austria and FAO,
598 Rome, Italy.
- 599 Jiang Y., Zhang L., Zhang B., et al. (2016). "Modeling irrigation management for water conservation by
600 DSSAT-maize model in arid northwestern China." *Agricultural Water Management* 177: 37-45.
- 601 Jones J., Hoogenboom G., Porter C., et al. (2003). "The DSSAT cropping system model." *European
602 Journal of Agronomy* 18 (3-4): 235-265.
- 603 Kang S., Zhang L., Liang Y., et al. (2002). "Effects of limited irrigation on yield and water use efficiency
604 of winter wheat in the Loess Plateau of China." *Agricultural Water Management* 55 (3): 203-216.
- 605 Keating B., Carberry P., Hammer G., et al. (2003). "An overview of APSIM, a model designed for
606 farming systems simulation". *European Journal of Agronomy* 18 (3-4): 267-288.

607 Kendy E., Molden D., Steenhuis T., et al. (2003). Policies drain the North China Plain: agricultural policy
608 and groundwater depletion in Luancheng County, 1949-2000. Colombo, Sri Lanka: International
609 Water Management Institute (IWMI). (IWMI Research Report 71) [doi: 10.3910/2009.074]

610 Knorzer H., Grozinger H., Graeff-Honninger S., et al. (2011). "Integrating a simple shading algorithm
611 into CERES-wheat and CERES-maize with particular regard to a changing microclimate within a
612 relay-intercropping system." *Field Crops Research* 121 (2): 274-285.

613 Konikow L. and Kendy E. (2005). "Groundwater depletion: A global problem." *Hydrogeology Journal*
614 13(1): 317-320.

615 Li J., Inanaga S., Li Z., et al. (2005). "Optimizing irrigation scheduling for winter wheat in the North
616 China Plain." *Agricultural Water Management* 76 (1): 8-23.

617 Li Y., Huang H., Ju H., et al. (2015). "Assessing vulnerability and adaptive capacity to potential drought
618 for winter-wheat under the RCP 8.5 scenario in the Huang-Huai-Hai Plain." *Agriculture,
619 Ecosystems & Environment* 209: 125-131.

620 Luo J., Shen Y., Qi Y., et al. (2018). "Evaluating water conservation effects due to cropping system
621 optimization on the Beijing-Tianjin-Hebei plain, China" *Agricultural Systems* 159: 32-41.

622 Lv L., Yao Y., Zhang L., et al. (2013). "Winter wheat grain yield and its components in the North China
623 Plain: irrigation management, cultivation, and climate." *Chilean Journal of Agricultural Research*
624 73 (3): 233-242.

625 Meng Q., Sun Q., Chen X., et al. (2012). "Alternative cropping systems for sustainable water and nitrogen
626 use in the North China Plain." *Agriculture, Ecosystems & Environment* 146 (1): 93-102.

627 Meng Q., Wang H., Yan P., et al. (2017). "Designing a new cropping system for high productivity and
628 sustainable water usage under climate change." *Scientific Reports* 7.

629 Mo X., Lin Z. and Liu S. (2006). "Spatial-temporal Evolution and Driving Forces of Winter Wheat
630 Productivity in the Huiang-Huai-Hai Region." *Journal of Natural Resources* 21 (3): 449-457.

631 Moiwo J., Lu W., Zhao Y., et al. (2010). "Impact of land use on distributed hydrological processes in the
632 semi-arid wetland ecosystem of Western Jilin." *Hydrological Processes* 24 (4): 492-503.

633 Moiwo J., Yang Y., Li H., et al. (2009). "Comparison of GRACE with in situ hydrological measurement
634 data shows storage depletion in Hai River basin, Northern China." *Water SA* 35: 663-670.

635 Nakayama T., Yang Y., Watanabe M., et al. (2006). "Simulation of groundwater dynamics in the North
636 China Plain by coupled hydrology and agricultural models." *Hydrological Processes* 20 (16):
637 3441-3466.

638 Nyberg A., Rozelle S. (1999). *Accelerating China's rural transformation*. Washington, D.C.: World Bank,
639 Washington, D.C.

640 Pei H., Scanlon R., Shen Y., et al. (2015). "Impacts of varying agricultural intensification on crop yield
641 and groundwater resources: comparison of the North China Plain and US High Plains." *642 Environmental Research Letters* 10 (4): 044013.

643 Portmann F., Siebert S. and Döll P. (2010). "MIRCA2000—Global monthly irrigated and rainfed crop
644 areas around the year 2000: A new high-resolution data set for agricultural and hydrological
645 modeling." *Global Biogeochemical Cycles* 24, GB 1011, doi:10.1029/2008GB003435..

646 Ritchie J., (1985). *A User-Orientated Model of the Soil Water Balance in Wheat*. Wheat Growth and
647 Modelling. W. Day and R. K. Atkin. Boston, MA, Springer US: 293-305.

648 Shen Y., Kondoh A., Tang C., et al. (2002). "Measurement and analysis of evapotranspiration and surface
649 conductance of a wheat canopy." *Hydrological Processes* 16 (11): 2173-2187.

650 Shu Y., Villholth K., Jensen K., et al. (2012). "Integrated hydrological modeling of the North China Plain:
651 Options for sustainable groundwater use in the alluvial plain of Mt. Taihang." *Journal of
652 Hydrology* 464: 79-93.

653 Sun C. and Ren L. (2013). "Assessment of surface water resources and evapotranspiration in the Haihe
654 River basin of China using SWAT model." *Hydrological Processes* 27 (8): 1200-1222.

655 Sun H., Zhang X., Wang E., et al. (2015). "Quantifying the impact of irrigation on groundwater reserve
656 and crop production – A case study in the North China Plain." *European Journal of Agronomy* 70
657 (Supplement C): 48-56.

658 Sun Q., Krobel R., Muller T., et al. (2011). "Optimization of yield and water-use of different cropping
659 systems for sustainable groundwater use in North China Plain." *Agricultural Water Management*
660 98 (5): 808-814.

661 Tian Z., Zhong H., Shi R., et al. (2012). "Estimating potential yield of wheat production in China based
662 on cross-scale data-model fusion." *Frontiers of Earth Science* 6 (4): 364-372.

663 Tian Z., Zhong H., Sun L., et al. (2014). "Improving performance of Agro-Ecological Zone (AEZ)
664 modeling by cross-scale model coupling: An application to japonica rice production in Northeast
665 China." *Ecological Modelling* 290 (0): 155-164.

666 Tubiello F. and Fischer G. (2007). "Reducing climate change impacts on agriculture: Global and regional
667 effects of mitigation, 2000-2080." *Technological Forecasting and Social Change* 74 (7): 1030-
668 1056.

669 van Oort P. A. J., Wang G., Vos J., et al. (2016). "Towards groundwater neutral cropping systems in the
670 Alluvial Fans of the North China Plain." *Agricultural Water Management* 165: 131-140.

671 Wang J., Huang J., Rozelle S., et al. (2009). "Understanding the Water Crisis in Northern China: What the
672 Government and Farmers are Doing." *International Journal of Water Resources Development* 25
673 (1): 141-158.

674 Wang J., Wang E., Yang X., et al. (2012). "Increased yield potential of wheat-maize cropping system in
675 the North China Plain by climate change adaptation." *Climatic Change* 113 (3-4): 825-840.

676 Wang J., Zhang L. and Huang J. (2016). "How could we realize a win-win strategy on irrigation price
677 policy? Evaluation of a pilot reform project in Hebei Province, China." *Journal of Hydrology*
678 539: 379-391.

679 Wang X., Li X., Fischer G., et al. (2015). "Impact of the changing area sown to winter wheat on crop
680 water footprint in the North China Plain." *Ecological Indicators* 57: 100-109.

681 Webber M., Barnett J., Finlayson B., et al. (2008). "Pricing China's irrigation water." *Global*
682 *Environmental Change* 18 (4): 617-625.

683 Weedon G. P., Balsamo G., Bellouin N., et al. (2014). "The WFDEI meteorological forcing data set:
684 WATCH Forcing Data methodology applied to ERA-Interim reanalysis data." *Water Resources*
685 *Research* 50 (9): 7505-7514.

686 Wu Q. and Xie H. (2017). "A Review and Implication of Land Fallow System Research." *Journal of*
687 *Resources and Ecology* 8 (3): 223-231.

688 Xiao D., Shen Y., Qi Y., et al. (2017). "Impact of alternative cropping systems on groundwater use and
689 grain yields in the North China Plain Region." *Agricultural Systems* 153: 109-117.

690 Yang X., Chen Y., Pacenka S., et al. (2015). "Recharge and Groundwater Use in the North China Plain
691 for Six Irrigated Crops for an Eleven Year Period." *PLOS ONE* 10 (1): e0115269.

692 Yang Y., Watanabe M., Zhang X., et al. (2006). "Estimation of groundwater use by crop production
693 simulated by DSSAT-wheat and DSSAT-maize models in the piedmont region of the North
694 China Plain." *Hydrological Processes* 20 (13): 2787-2802.

695 Yang Y., Yang Y., Moiwo J. P., et al. (2010). "Estimation of irrigation requirement for sustainable water
696 resources reallocation in North China." *Agricultural Water Management* 97 (11): 1711-1721.

697 Yuan Z. and Shen Y. (2013). "Estimation of Agricultural Water Consumption from Meteorological and
698 Yield Data: A Case Study of Hebei, North China." *PLOS ONE* 8 (3): e58685.

699 Zhang Y., Shen Y., Sun H., et al. (2011). "Evapotranspiration and its partitioning in an irrigated winter
700 wheat field: A combined isotopic and micrometeorologic approach." *Journal of Hydrology* 408
701 (3): 203-211.

702 Zhang Z., Fei Y., and Chen Y., ET AL. (2009). "Evolution and development of groundwater environment
703 in North China Plain under human activities." Beijing, Geological Publishing House.

704 Zhang Q.S., Zhang X. 1995. Water issues and sustainable social development in China. *Water*
705 *International*, 20(3): 122-128.

706 Zhong H., Sun L., Fischer G., et al. (2017). "Mission Impossible? Maintaining regional grain production
707 level and recovering local groundwater table by cropping system adaptation across the North
708 China Plain." *Agricultural Water Management* 193: 1-12.

709 Zaveri E., Grogan D., Fisher-Vanden K., et al. (2016). "Invisible water, visible impact: groundwater use
710 and Indian agriculture under climate change." *Environmental Research Letters* 11(8): 084005.
711 doi:10.1088/1748-9326/11/8/084005.
712

713
714

Table 1. Genetic coefficients of local wheat, summer maize and early maize

Winter Wheat		Summer Maize		Early Maize	
Parameter	Value	Parameter	Value	Parameter	Value
PIV	1.5	P1	300	P1	277
P1D	2.4	P2	0.3	P2	1.05
P5	-6.0	P5	640	P5	787
G1	3.9	G2	740	G2	711
G2	3.0	G3	14	G3	10.0
G3	2.9	PHINT	60	PHINT	48
PHINT	90				

715 Note: (1) Wheat: P1V: vernalization; P1D: photoperiod sensitivity; P5: grain filling duration; G1: kernel number; G2:
716 kernel weight; G3: spike number; PHINT: phyllochron interval. (2) Maize: P1: duration of the juvenile phase; P2:
717 photoperiod sensitivity; P5: duration of the reproductive phase; G2: kernel number; G3: kernel growth rate; PHINT:
718 phyllochron interval. See Jones et al. (2003) for technical details.

719 Source: Yang et al., (2006) and Zhong et al., (2017).

720
721
722

723 Table 2. ET of wheat, maize and all other crops, vegetables and fruit trees combined in the three plains

Plain	Wheat		Maize		Others	
	10 ⁶ m ³	% of existing total ET	10 ⁶ m ³	% of existing total ET	10 ⁶ m ³	% of existing total ET
Piedmont plain	2808.61	31.74	2139.02	24.17	3900.59	44.08
Central plain	4242.48	27.00	3487.24	22.19	7985.42	50.81
Coastal plain	495.31	19.91	489.39	19.67	1502.69	60.41
Total	7546.40	27.90	6115.64	22.61	13388.70	49.49

724
725
726
727
728

Table 3. Areas for winter wheat fallow and potential WM-R cropping

	Winter fallow area		WM-R cropping area	
	10 ³ ha	% of existing wheat area	10 ³ ha	% of existing WM-S area
Piedmont plain	-319.92	-44.78	394.54	71.50
Central plain	-377.37	-36.15	666.59	75.66
Coastal plain	-39.15	-32.76	80.35	68.05
Total	-736.44	-39.22	1141.47	73.26

729
730

731
732
733

Table 4. Changes in wheat and maize production under the adapted cropping systems

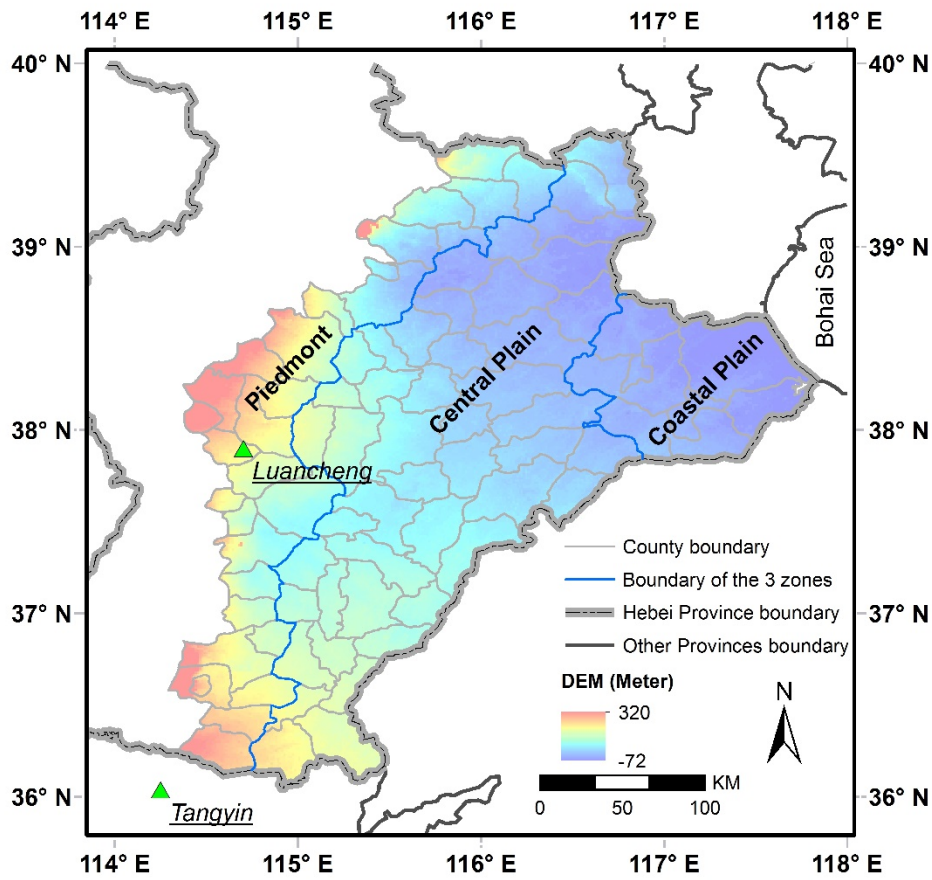
	Wheat		Maize		Total	
	10 ³ ton	% of existing total production	10 ³ ton	% of existing total production	10 ³ ton	% of existing total production
Piedmont plain	-2469.74	-44.57	1083.53	35.27	-1386.21	-16.09
Central plain	-2859.09	-36.02	1688.41	36.61	-1170.68	-9.32
Coastal plain	-282.13	-32.95	233.18	32.63	-48.95	-3.24
Total	-5610.96	-39.14	3005.13	36.04	-2605.83	-11.49

734
735
736
737
738

Table 5. Changes in Irrigation Water Requirement of wheat, maize, and the whole cropping sector under the adapted cropping systems

	Wheat		Maize		Total	
	10 ⁶ m ³	% of existing wheat IWR	10 ⁶ m ³	% of existing maize IWR	10 ⁶ m ³	% of existing total IWR
Piedmont plain	-931.05	-63.47	102.18	29.89	-828.86	-45.82
Central plain	-1588.87	-60.92	201.17	40.71	-1387.70	-44.73
Coastal plain	-118.97	-42.09	13.60	23.14	-105.36	-30.86
Total	-2638.88	-60.56	316.95	35.42	-2321.93	-44.20

739



740

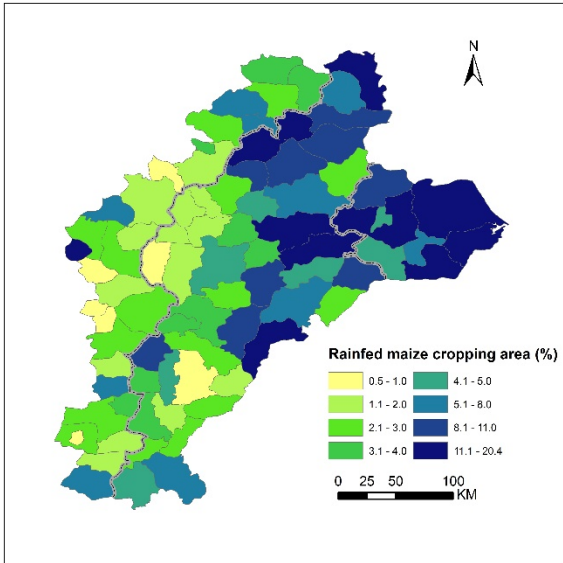
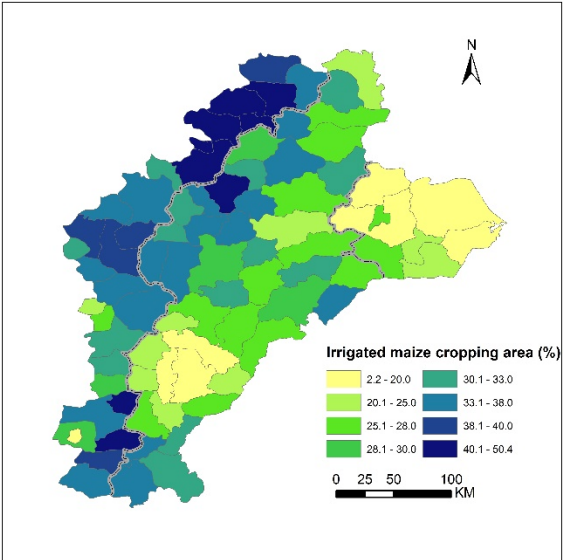
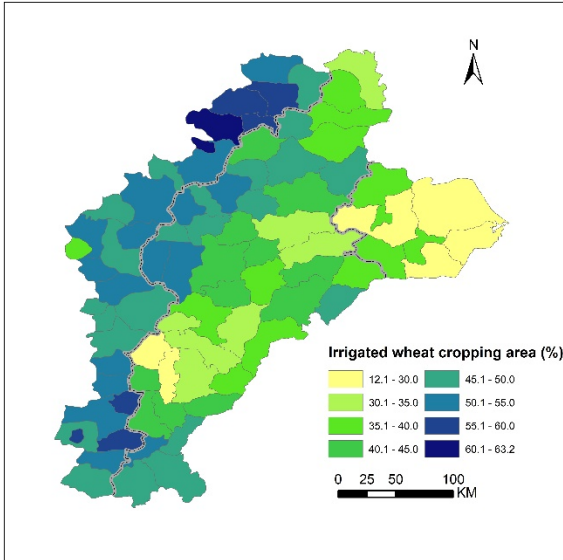
741

Figure 1. The Hebei Plain

742

743

744

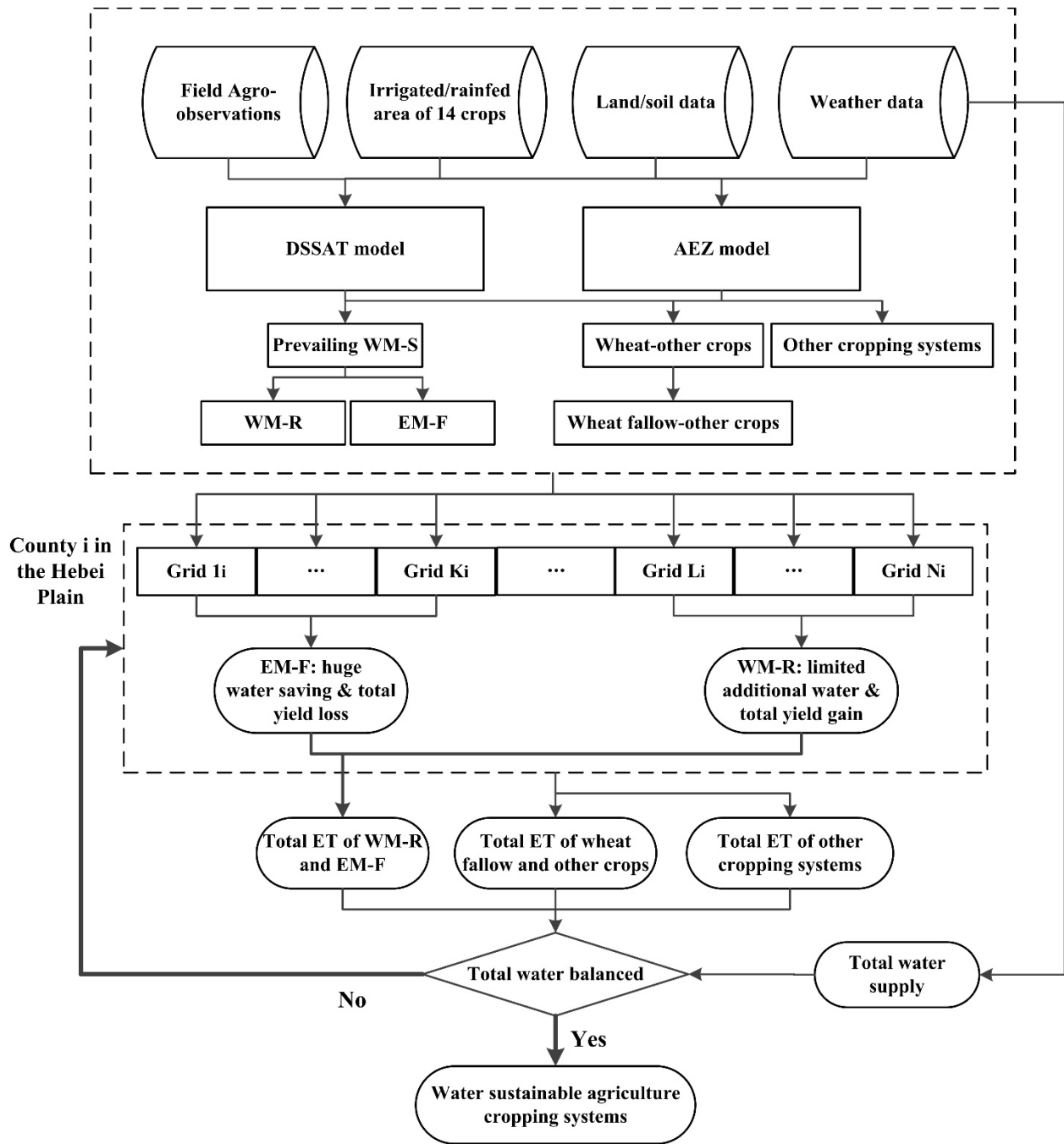


745

746

747 Figure 2. The shares of irrigated wheat, irrigated and rainfed maize cropping area in the county's total cropland
 748 across the Hebei Plain

749



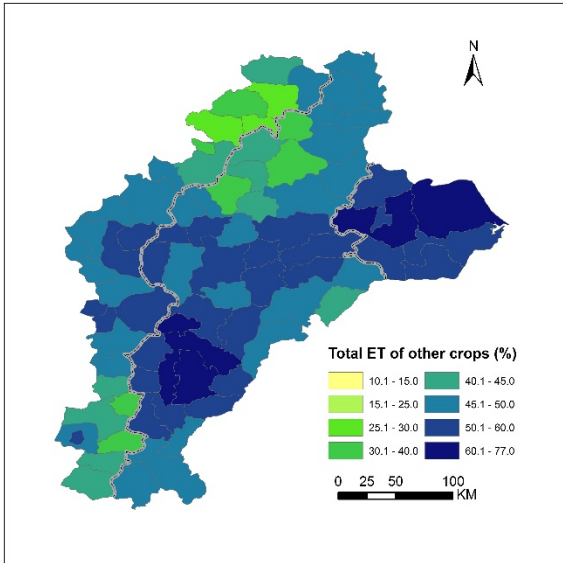
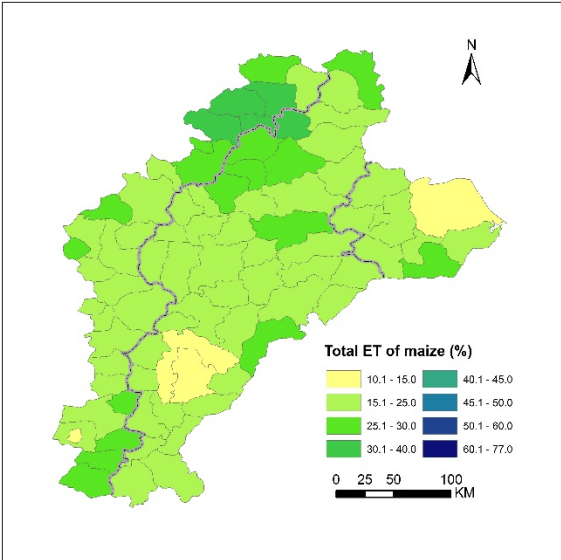
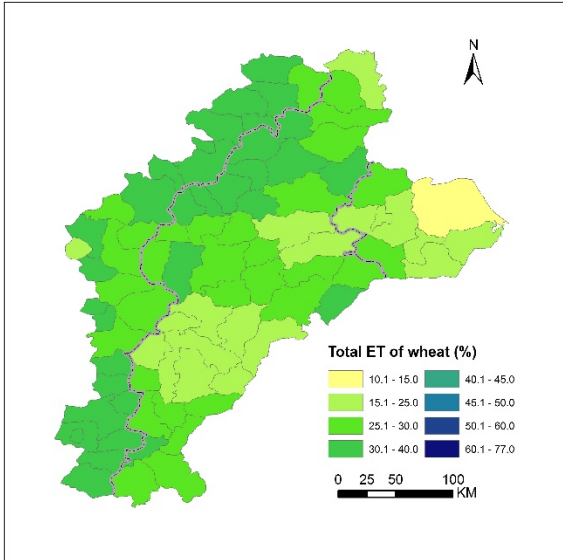
750

751

752

753

Figure 3. Regional cropping systems adaptation strategy: flow chart



754

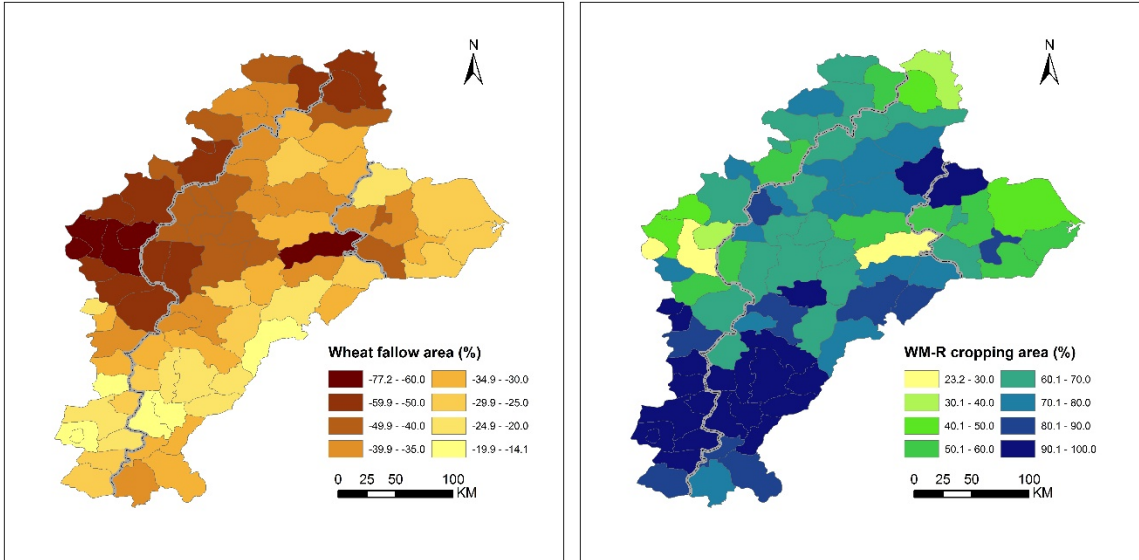
755

756

757

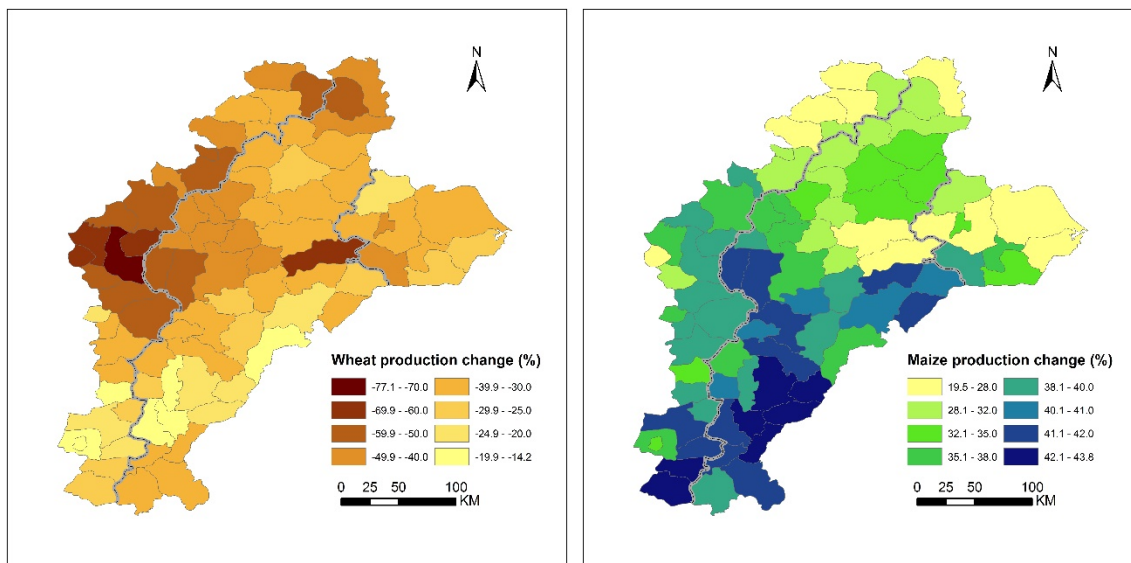
758

Figure 4. ET share of wheat, maize and the combination of all other crops, vegetables, and fruit trees in the total ET at the county level in the Hebei Plain

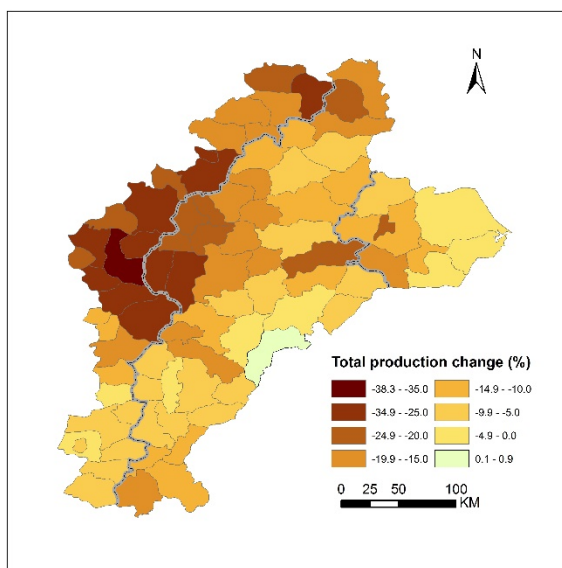


759
 760 Figure 5. The share of wheat fallow area in the existing wheat area (left) and the share of potential WM-R cropping
 761 area in the existing WM-S area (right) at the county level in the Hebei Plain
 762

763
764



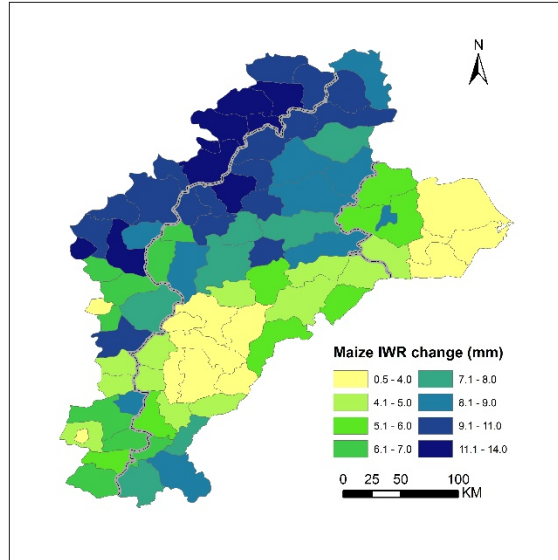
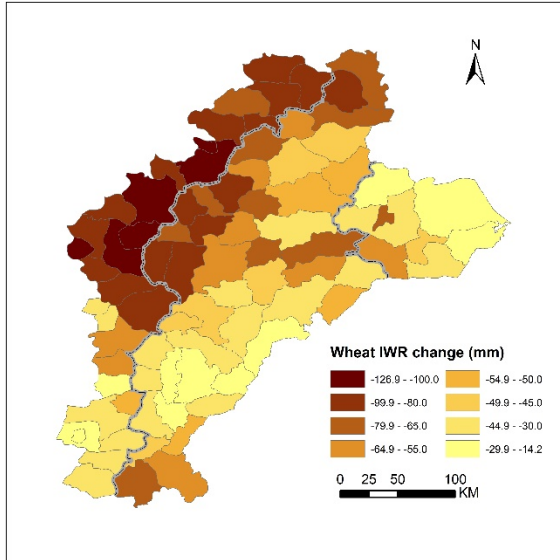
765



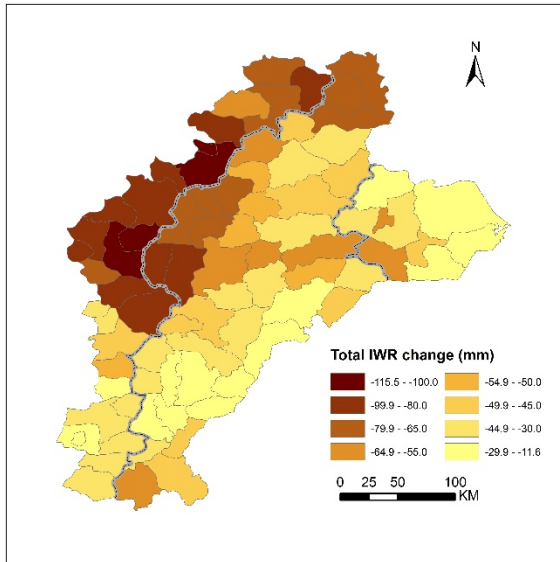
766

767 Figure 6. Changes in total production of wheat, maize and total grain at the county level in the Hebei Plain

768



769



770

771 Figure 7. Changes in Irrigation Water Requirement (IWR) of wheat, maize, and the whole cropping sector at the

772 county level in the Hebei Plain

773